Robust Particle Swarm Optimization of RFMs for High-Resolution Satellite Images Based on K-Fold Cross-Validation

Saeid Gholinejad, Amin Alizadeh Naeini, and AliReza Amiri-Simkooei

***Abstract*—Rational function model (RFM) is one of the most popular methods of geometrically correcting high-resolution satellite images (HRSIs). This model encounters overparameterization problem due to the existence of highly correlated RFM coefficients, namely, rational polynomial coefficients (RPCs). Recently, a number of methods have been proposed based on particle swarm optimization (PSO) to find the optimal RPCs. Although these algorithms are useful for determining the optimal RPCs, their results are strongly influenced by changes in both initial values and ground control points (GCPs) distribution. To address this problem, this study proposes a modified version of PSO based on the k-fold cross-validation, known as PSO-KFCV, which works well even in the presence of limited GCPs. To evaluate the performance of the proposed method, four different HRSIs were used. Our experimental results indicate that PSO-KFCV is indeed robust against the initial values and GCPs distribution. In addition, the experiments demonstrated that the proposed method led to significant improvement with respect to state-of-the-art meta-heuristic methods.**

***Index Terms*—High resolution satellite images (HRSIs), k-fold cross-validation (KFCV), particle swarm optimization (PSO), rational function model (RFM).**

I. Introduction

RECENTLY, a wide range of high-resolution satellite images (HRSIs) has provided the opportunity to extract geospatial information from the earth's surface for different remote sensing applications [1], [2]. This extraction is performed through different transformations from the image space to object space. At present, all HRSIs are provided with coefficients of the rational function model (RFM), known as rational polynomial coefficients (RPCs). Accordingly, RFM is the most frequently used transformation for georeferencing of HRSIs. However, due to a number of highly correlated RPCs, RFM suffers from the ill-posedness problem [3]–[6]. To tackle this problem, l_0, l_1, and l_2 norm regularization methods have been used in the literature.

The l_2 regularization approach, which does not ignore any RFM parameters, tries to handle the magnitude of the coefficients vector by imposing some additional terms to the objective function of the RFM problem. In this category, L-curve based ridge estimation [7], iteration by correcting characteristic value [8], the Levenberg–Marquardt algorithm (LM) [9], and a method based on the LM and orthogonal transformation of error equation coefficient matrix [10] are some of the most important l_2 regularization-based studies employed to estimate RPCs.

Unlike the l_0 regularization, l_1 regularization attains a sparse result, which is a vector with only a few nonzero elements. To the authors' best knowledge, L1LS [5] is the only l_1-based regularization framework in the literature that tries to find the optimum number and values of RPCs through a convex formulation of the RFM problem.

Essentially, there is no need to involve all the terms in the RFM, as some of them are inconsistent with the nature of the distortions [4]. Consequently, it seems necessary to remove some of the terms in the transformation process. The l_0 regularization-based approaches try to reduce the number of terms in the RFM, improving the results of the image-to-object transformation. Directly removing the third-order terms [11], omitting some unnecessary parameters based on the scatter matrix and elimination transformation strategy [12], Nested regression based optimal selection [13], and uncorrelated and statistically significant RFM [14] are some examples of the l_0 regularization using an exhaustive search strategy.

The problem of finding the optimal RPCs through the l_0 norm optimization is an NP-hard one and does not have a solution with a polynomial order computational complexity. Therefore, the meta-heuristic methods, which consciously search the solution space, seem to be useful in solving such a problem. Genetic algorithm (GA) [15] and particle swarm optimization (PSO) [16] are the two most frequently used methods in this field. GA and its modified version were employed on the RFM in [3] and [17], respectively. Conventional PSO [18] and its modified version, known as PSO specialized for RFM optimization (PSORFO) [4], were presented to find the optimal number and combination of RFM parameters. In another study, PSORFO was improved by figure condition analysis, named FCA-PSO [6]. This method uses the digital elevation model (DEM) of the image scene. It should be mentioned that PSO has outperformed GA in terms of computational time and accuracy [4], [18].

Although PSO-based methods [4], [6] can effectively determine the number of optimal parameters in RFM, they are highly dependent on the distribution of control points (CPs) and the initial values to start the algorithm. The above two factors

Manuscript received July 23, 2018; revised September 24, 2018 and October 22, 2018; accepted October 31, 2018. Date of publication December 10, 2018; date of current version September 16, 2019. *(Corresponding author: Amin Alizadeh Naeini).*

The authors are with the Department of Geomatics Engineering, Faculty of Civil Engineering and Transportation, University of Isfahan, Isfahan 8174673441, Iran (e-mail: Saeid.Gholinejad@trn.ui.ac.ir; a.alizadeh@eng.ui.ac.ir; amiri@eng.ui.ac.ir).

Color versions of one or more of the figures in this paper are available online at http://ieeexplore.ieee.org.

Digital Object Identifier 10.1109/JSTARS.2018.2881382

lead the PSO-based algorithms to different solutions in different runs, reducing the reliability of the algorithms [6]. Such methods require CPs that are generally categorized in three groups: ground CPs (GCPs), dependent check points (DCPs) and independent check points (ICPs) [6]. RPCs are determined using GCPs and the cost value for each particle is assessed by calculating the root mean squares error (RMSE) over DCPs through a cost function (CF). Finally, the accuracy of the methods is obtained through calculating RMSE over ICPs. Choosing GCPs and DCPs directly influence the determination of the optimal RPCs. In previous studies, GCPs and DCPs were selected either by users or randomly. This kind of partitioning increases the probability of falling into local minima while using PSO. In the meantime, the final results of the meta-heuristic methods, such as PSO, completely depend on the CF. Therefore, different GCPs distributions may lead to different results.

Focusing on this problem, for the first time, a stable method based on the integration of PSO and k-fold cross-validation, known as PSO-KFCV, is proposed in this study to reduce the impact of the GCPs distribution and initial values on the determination of the optimal RPCs. In this method, *k*-folds are constructed over the set of training points, GCPs and DCPs. For each particle, RMSE is calculated over DCPs in all *k*-folds. Subsequently, the highest amount of RMSE is assigned to the particle as the cost value. Each particle then has its worst cost value. Lower cost values are thus assigned to those particles that have low RMSE on any distribution of GCPs. In addition to its stability, the proposed method inherently considers different data distributions and accordingly finds the coefficients that are optimal under all conditions. Therefore, the cost value is calculated in the worst possible manner. This pessimistic consideration forces the algorithm to find the optimal particle in different situations. This factor increases the results precision and stability at the same time. The main contributions of this study are summarized as follows: 1) the PSO algorithm has been combined with the concept of KFCV to address RFM's ill-posedness and 2) a stable method has been proposed based on the GCPs' distribution.

The rest of this study is organized in the following manner. The preliminaries for the RFM and PSO, along with the methodology of the proposed PSO-KFCV, are introduced in Section II. The experimental results and discussion are described in Section III. We conclude this study in Section IV.

II. Methodology

A. Rational Function Model

RFM consists of two mathematical equations that establish the spatial relationship between the ground space and the image space. Each of these equations is a ratio of two third-order polynomial functions in the form of

$$l = \frac{P_1(X,Y,Z)}{P_2(X,Y,Z)} \tag{1}$$

$$s = \frac{P_3(X,Y,Z)}{P_4(X,Y,Z)} \tag{2}$$

where

$$\begin{aligned} P_1(X,Y,Z) = {} & a_1 + a_2X + a_3Y + a_4Z \\ & + a_5XY + a_6XZ + a_7YZ + a_8X^2 \\ & + a_9Y^2 + a_{10}Z^2 + a_{11}YXZ + a_{12}X^3 \\ & + a_{13}XY^2 + a_{14}XZ^2 + a_{15}X^2Y + a_{16}Y^3 \\ & + a_{17}YZ^2 + a_{18}X^2Z + a_{19}Y^2Z + a_{20}Z^3 \end{aligned} \tag{3}$$

$$P_2 = b_1 + b_2X + b_3Y + b_4Z + \cdots + b_{20}Z^3 \tag{4}$$

$$P_3 = c_1 + c_2X + c_3Y + c_4Z + \cdots + c_{20}Z^3 \tag{5}$$

$$P_4 = d_1 + d_2X + d_3Y + d_4Z + \cdots + d_{20}Z^3 \tag{6}$$

where l and s are normalized lines and samples of the points in the image space and X, Y, and Z are their corresponding normalized coordinates in the ground space [19]. a_i, b_i, c_i, and $d_i (i = 1, , 20)$, which comprise 80 parameters in total, are known as RPCs. Among these 80 parameters, b_1 and d_1 are dependent parameters and are usually set as $b_1 = d_1 = 1$. Therefore, 78 independent parameters remain for the optimization step.

Essentially, these nonlinear equations are linearized as follows:

$$P_1(X,Y,Z) - lP_2(X,Y,Z) = 0 \tag{7}$$

$$P_3(X,Y,Z) - sP_4(X,Y,Z) = 0. \tag{8}$$

Then, by using n GCPs, the above equations can be reformed as follows:

$$y = Ax + e \tag{9}$$

where $A \in R^{2n\times 78}$, $y \in R^{2n\times 1}$, and $e \in R^{2n\times 1}$ are the coefficient matrix, the observations vector, and the residuals vector, respectively. Additionally, $x \in R^{78\times 1}$ is a vector containing the RFM parameters. The least-squares solution for (9) is as follows:

$$x = (A^TA)^{-1}A^Ty. \tag{10}$$

B. Particle Swarm Optimization

PSO, which is essentially a continuous search strategy, is an intelligent computational algorithm based on the movement of organisms in a bird flock or fish school. PSO tries to optimize a problem by iteratively improving a candidate solution according to a CF [16]. In this method, after generating the initial population, the best particle ($gBest$) and the best memory of each particle ($lBest$) are calculated. During repetitions of the PSO algorithm, the particle velocity (V_i^{k+1}) is updated using its current velocity(V_i^k), its current position (P_i^k), $lBest$, and $gBest$ as follows:

$$V_i^{k+1} = \omega(k)V_i^k + c_1r_1(lBest - P_i^k) + c_2r_2(gBest - P_i^k) \tag{11}$$

where k is the current repetition, r_1 and r_2 are two uniform random values, and c_1 and c_2 are two constant acceleration values. $\omega(k)$ is the time-varying inertia weight function, which

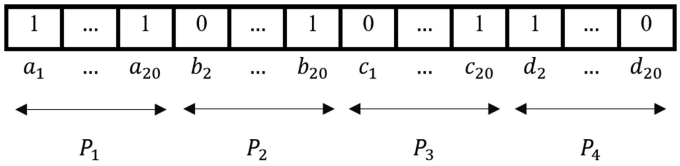

Fig. 1. Structure of the particle used in PSO-KFCV.

is defined in the same way as defined in [4] in the following form:

$$\omega(k) = \omega_{\min} + (\omega_{\max} - \omega_{\min})\frac{k_{\max} - k}{k} \tag{12}$$

where $\omega_{\max}$ and $\omega_{\min}$ are the maximum and the minimum values for the inertia weight function and $k_{\max}$ is the number of iterations. After updating the velocity of the particles, their positions are as follows:

$$P_i^{k+1} = P_i^k + V_i^{k+1}. \tag{13}$$

C. PSO With KFCV for Estimation of RPCs

As discussed previously, l_0 regularization attempts to remove highly correlated RPCs from the RFM's structure. In previous studies [4], [6], only a few RPCs were considered, while a large number of these coefficients were eliminated prior to entering the optimization step. This kind of elimination conflicts with the nature of the RFM. As a result, in this study, all the 78 parameters are considered in the optimization phase.

In this study, as in the previous relevant studies [4], [6], a binary version of the PSO algorithm has been used to estimate the optimal number of RPCs. Each particle shows a combination of RFM parameters in a string of 78 binary values. As illustrated in Fig. 1, each of the particle values is assigned to one of the RPCs. In this figure, "1" means the corresponding RPC contributes to the RFM, whereas "0" means the opposite.

The RMSE over DCPs was usually considered to be CF in such problems [4], [6], [17]. This may result in a downward-biased estimation of RPCs, because a particle may have low RMSE just for a special distribution of DCPs. To tackle this problem, this study proposes a KFCV based CF. The KFCV is a technique utilized for generalizing the results of statistical analysis in a data set. In the KFCV, data are first partitioned into k subsets of an equal (or nearly equal) size. Then, modeling is performed in k iterations so that within each iteration, a subset is selected for validation while the remaining $k-1$ subsets are used for estimation [20]. The most preferred KFCV methods are 5-fold and 10-fold cross-validations [21]. Out of these two cross-validation techniques, we used 5-fold cross-validation to be able to work well with limited GCPs.

Therefore, based on the above reasoning, instead of separating GCPs and DCPs, they are combined together and partitioned into five folds. For each particle, the ordinary least squares (OLS) is performed in five iterations. In each iteration, one of the folds is considered to be DCPs, whereas the remaining folds apply to estimate RPCs through the OLS. Among five RMSEs, calculated from five iterations of the OLS, the highest RMSE is selected as the cost value of the particle. This procedure forces the PSO to find the solution that has an appropriate RMSE for any distribution of CPs.

TABLE I
EXPERIMENTAL DATA SETS USED IN THIS STUDY

Data Set	Satellite	Location	GSD (m)	Data Size (m)	Number of CPs
Geo-ISF	GeoEye-1	Isfahan Province, Iran.	0.5	800×600	70
PL-ISF	Pleiades	Isfahan Province, Iran.	0.5	650×700	70
WV-ISF	Worldview-3	Isfahan Province, Iran.	0.41	400×300	65
Geo-URM	GeoEye-1	Urmia, West Azerbaijan Province, Iran.	0.5	4700×14800	60

III. EXPERIMENTS

Four remotely sensed images, acquired by three HRSIs, were used in this study. Detailed information about these data sets has been presented in Table I.

Two relevant competing methods, PSORFO [4] and FCA-PSO [6], were used. These two methods, like our proposed method, try to tackle RFM's ill-posedness by selecting optimum coefficients of RFM. However, they work on a specific form of RFM that has only 32 coefficients. In this kind of RFM, 1) the denominators are considered the same and 2) the third-order coefficients are ignored, except for a_{11} and c_{11}. However, in this study, we work with the common version of RFM that has 78 parameters; as a result, all methods including PSORFO, FCA-PSO, and PSO-KFCV try to find the optimum coefficients of this type of RFM, which is frequently used in the remote sensing community.

PSORFO is a modified version of PSO in which a $tanh$ function has been used instead of the sigmoid function to improve the estimation of RFM coefficients. FCA-PSO imposes figure condition analysis on the CF of the PSO, in which the sum of estimated errors for all the pixels of the image is regarded as the cost value.

With regard to the parameter setting, it should be mentioned that the PSO's parameters in all methods (i.e., PSORFO, FCA-PSO, and PSO-KFCV) are set as described in [4]. FCA-PSO also requires the DEM. To do this, as recommended in [6], ASTER global DEM (GDEM)[1] was used. It should be noted that PSORFO and PSO-KFCV require some DCPs to determine the cost value of the particles, while FCA-PSO does not require DCPs for cost value computation. For PSORFO and PSO-KFCV methods, in all experiments, 20% of the GCPs were assigned as DCP.

The quality assessment of the results is performed with two evaluating metrics: 1) RMSE and 2) standard deviation (STD). RMSE is calculated over ICPs and determines the accuracy of the obtained results. STD, which is calculated over RMSEs, is a proper measure of stability.

In the following, the experiments have been divided into two sections. In the first section, the sensitivity of the PSO-KFCV to changing both initial values and GCPs' distribution is analyzed, along with the competing methods. The computational times of the considered methods have been studied in the second section.

[1] http://earthexplorer.usgs.gov

TABLE II
RESULTS OBTAINED FROM IMPLEMENTING DIFFERENT METHODS ON FIVE DATA SAMPLES OF THE GEO-ISF DATA SET

Data sample	Avg-RMSE (in pixel)			STD-RMSE (in pixel)		
	PSORFO	FCA-PSO	PSO-KFCV	PSORFO	FCA-PSO	PSO-KFCV
1	2.6039	1.0899	**0.7998**	2.4770	**0.0952**	0.2135
2	0.9645	0.8542	**0.7294**	0.7233	0.1162	**0.0398**
3	1.0329	0.8948	**0.6401**	0.6003	0.1011	**0.0276**
4	0.6548	0.6271	**0.5702**	0.1103	0.0859	**0.0654**
5	3.3787	0.8060	**0.6477**	5.9703	0.1349	**0.0682**
Average	1.7270	0.8544	**0.6774**	1.9763	0.1066	**0.0829**

TABLE III
RESULTS OBTAINED FROM IMPLEMENTING DIFFERENT METHODS ON FIVE DATA SAMPLES OF THE PL-ISF DATA SET

Data sample	Avg-RMSE (in pixel)			STD-RMSE (in pixel)		
	PSORFO	FCA-PSO	PSO-KFCV	PSORFO	FCA-PSO	PSO-KFCV
1	1.6877	0.8757	**0.7513**	0.7129	0.2787	**0.0552**
2	1.0428	**0.7928**	0.9417	0.1705	0.1632	**0.0829**
3	0.8210	0.9775	**0.7502**	0.0815	0.2626	**0.0422**
4	4.6203	0.9832	**0.8159**	8.3457	0.2925	**0.0674**
5	0.9265	1.0727	**0.7964**	0.1059	0.4599	**0.0419**
Average	1.8197	0.9404	**0.8111**	1.8833	0.2914	**0.0579**

TABLE IV
RESULTS OBTAINED FROM IMPLEMENTING DIFFERENT METHODS ON FIVE DATA SAMPLES OF THE WV-ISF DATA SET

Data sample	Avg-RMSE (in pixel)			STD-RMSE (in pixel)		
	PSORFO	FCA-PSO	PSO-KFCV	PSORFO	FCA-PSO	PSO-KFCV
1	3.3509	0.9622	**0.7695**	4.4733	0.1375	**0.0697**
2	1.4392	0.8158	**0.7793**	1.5284	0.1951	**0.0718**
3	1.1381	1.3392	**0.9202**	0.1789	0.3244	**0.0373**
4	1.8062	0.7741	**0.5856**	1.6185	0.2229	**0.0322**
5	4.6104	1.4493	**0.8216**	5.4348	0.3024	**0.0382**
Average	2.4690	1.0681	**0.7753**	2.6468	0.2364	**0.0498**

TABLE V
RESULTS OBTAINED FROM IMPLEMENTING DIFFERENT METHODS ON FIVE DATA SAMPLES OF THE GEO-URM DATA SET

Data sample	Avg-RMSE (in pixel)			STD-RMSE (in pixel)		
	PSORFO	FCA-PSO	PSO-KFCV	PSORFO	FCA-PSO	PSO-KFCV
1	2.0958	0.9478	**0.5922**	2.5415	1.1571	**0.0183**
2	2.2465	0.6178	**0.6079**	4.2286	**0.0050**	0.0130
3	1.5278	**0.6110**	0.6133	1.5066	**0.0065**	0.0166
4	1.9366	**0.5214**	0.5388	1.4171	**0.0019**	0.0255
5	0.5361	**0.5025**	0.5059	0.0297	**0.0060**	0.0098
Average	1.6686	0.6401	**0.5716**	1.9447	0.2353	**0.0167**

A. Sensitivity Analysis

The sensitivity, i.e., the accuracy and the stability of the PSO-KFCV to different initial values and GCPs distribution is discussed in this section. Meta-heuristic methods such as PSO are types of stochastic optimization methods, leading to different results in each run due to different initial values [22]. Accordingly, the stability of these methods must be assessed in every application. To do so, STDs of solutions of PSORFO, FCA-PSO, and PSO-KFCV are used, in which low STD indicates strong stability and vice versa. In the meantime, the sensitivity of the in-hand methods to the distribution of GCPs has been evaluated.

First, to verify the stability of the stated methods, each data set has been randomly divided into five data samples. As recommended in [23], 50 points of each data sample were considered as GCPs while the rest were considered as ICPs. In PSORFO and PSO-KFCV, 40 GCPs have been used to estimate RPCs while the rest are used for cost value calculation. However, in FCA-PSO, all the 50 points have been used for the estimation process of RPCs because particles cost value is calculated using GDEM's points.

For each data sample of each data set, PSORFO, FCA-PSO, and PSO-KFCV were performed ten times, leading to ten RMSEs. The average and STD of these ten RMSEs, referred to as *Avg-RMSE* and *STD-RMSE* from now on, were respectively considered the accuracy and the stability of each optimization method in the presence of different initial values. However, due to the use of five data samples coming from different GCPs' distribution, there are five *Avg-RMSE* and *STD-RMSE*. Accordingly, to comprehensively assess the sensitivity to the initial values, the average of five *Avg-RMSE*s and *STD-RMSE*s are considered, respectively, as the accuracy and the stability indicators. On the other hand, the average of the five *Avg-RMSE*s and *STD-RMSE*s can be also considered a metric for determining the sensitivity of the algorithms to GCPs' distribution. The obtained results of our experiments have been listed in Tables II–V, in which best values have been bolded.

According to Tables II–V, compared to PSORFO and FCA-PSO, PSO-KFCV has led to an average of 62.5% and 18% improvements in the RMSE values of the four data sets, respectively. Furthermore, unlike competing methods, PSO-KFCV has had subpixel accuracy in all cases. From the perspective of stability, the proposed method with the STD of 0.051 pixels on the average results of the four data sets leads to significant improvement compared to PSORFO and FCA-PSO. It can be said that the greatest achievement of our proposed method has been disclosed in analyzing STD values, which was in most cases lower than 0.1 pixels. In Fig. 2, we have tried to visually interpret the performance of the proposed method compared to competing methods. As is clear from this figure, the PSO-KFCV surpasses competing methods both in terms of precision and stability.

To assess the performance of the proposed method in the presence of limited GCPs, this study has evaluated the results of implementing PSO-KFCV, as well as PSORFO and FCA-PSO, with 10, 15, and 20 well-distributed GCPs. The corresponding experimental results have been presented in Table VI. As is clear from this table, from the accuracy point of view, in most cases the proposed method has had more accurate results than the two competing methods. With ten GCPs, PSO-KFCV has surpassed other methods in all the data sets, except for PL-ISF, in which the accuracies of all methods were the same. Precisely speaking, the RMSEs for PSO-KFCV have improved by 23% and 2% on average in the four data sets compared to PSORFO and FCA-PSO, respectively. Working with 15 GCPs, although both FCA-PSO and PSO-KFCV have had the best RMSE value in two

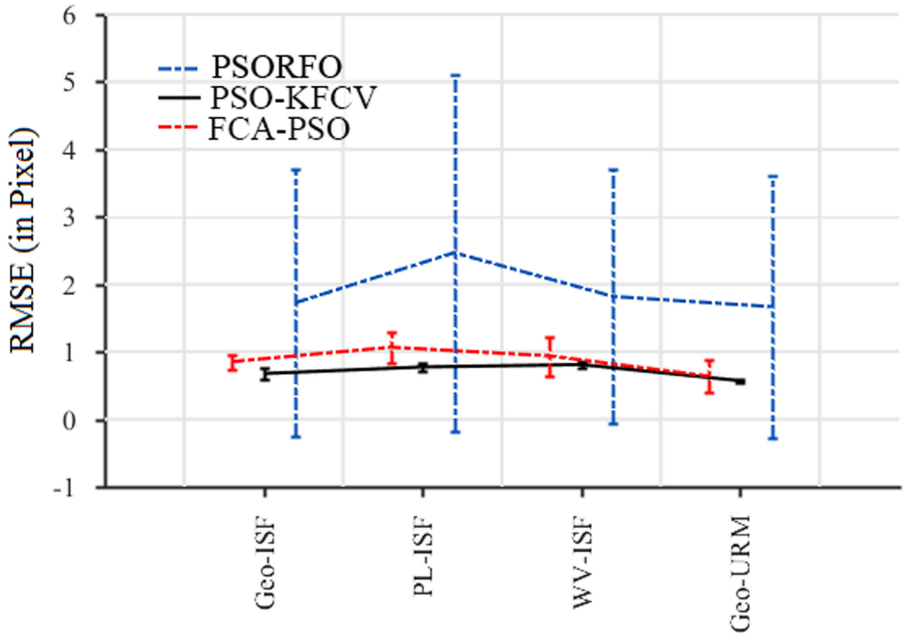

Fig. 2. RMSEs obtained from implementing different methods on the experimental data sets. *Avg-RMSE*s of methods are illustrated while the error-bars above and below the mean show the *STD-RMSE*.

TABLE VI
OBTAINED RESULTS FROM THE PSORFO, FCA-PSO, AND PSO-KFCV IN THE CASE OF LIMITED GCPS

Data Set	No. of GCPs/ICPs	Avg-RMSE (in pixel)			STD-RMSE (in pixel)		
		PSORFO	FCA-PSO	PSO-KFCV	PSORFO	FCA-PSO	PSO-KFCV
Geo-ISF	10/60	1.0645	0.8812	**0.8637**	2.7707	172.6970	**1.1309**
	15/55	0.8633	0.9192	**0.6542**	9.0681	**0.0879**	0.1211
	20/50	0.7171	0.6186	**0.5771**	3.5515	**0.1631**	0.1752
PL-ISF	10/60	**0.9385**	**0.9385**	**0.9385**	234.9982	235.0611	**2.8924**
	15/55	0.9868	**0.8885**	**0.8885**	21.1981	0.7836	**0.1876**
	20/50	1.0766	0.7796	**0.7470**	337.0709	**0.3297**	0.3620
WV-ISF	10/55	1.3068	0.7784	**0.7501**	42.9988	376.9984	**1.8388**
	15/50	1.9075	**0.7339**	0.7539	24.6069	**0.1977**	0.6910
	20/45	0.9366	0.8641	**0.7550**	37.4101	0.1641	**0.0990**
Geo-URM	10/50	0.7745	0.6079	**0.5969**	2828.8956	**1.8253**	6.4723
	15/45	0.7282	**0.5824**	**0.5824**	40.6754	0.7474	**0.0397**
	20/40	0.5651	0.5772	**0.5758**	19.7959	0.5060	**0.0029**

data set experiments (PL-ISF and Geo-URM), the improvement of PSO-KFCV has been 8%, on average in the four data sets, compared to FCA-PSO. In the case of 20 GCPs, our proposed PSO-KFCV has always outperformed PSORFO and FCA-PSO.

The most important achievement of our proposed method has been again demonstrated in the analysis of STD values in Table VI. PSO-KFCV has had subpixel STDs in all cases implemented by 15 and 20 GCPs. Furthermore, in the case of ten GCPs, PSORFO and FCA-PSO have had high STD values (more than 100 pixels in most cases), but our proposed method has reported 6.4723 pixels in the worst case. In summary, compared to the competing methods, better RMSE and STD values of the proposed method indicate its higher positional accuracy for the georeferencing of HRSIs than other methods, even in the case of limited GCPs.

B. Computational Time Analysis

In this part of our experiment, the average performance times of executing different methods on the experimental data sets are investigated. It is necessary to mention that all the experiments were carried out on a personal computer, the Intel Core i5 CPU at 2.53 GHz with 5.80 GB usable RAM.

Fig. 3 illustrates the average computational times of PSO-KFCV and the competing methods on the four different data sets. As demonstrated in Fig. 3, the computational time of FCA-PSO was significantly higher than other methods in three data sets: Geo-ISF, PL-ISF, and Geo-URM. This is because FCA-PSO uses DEM points in its CF, which dramatically increases its processing time. Another remarkable point is the lower computational time of FCA-PSO in comparison with PSO-KFCV

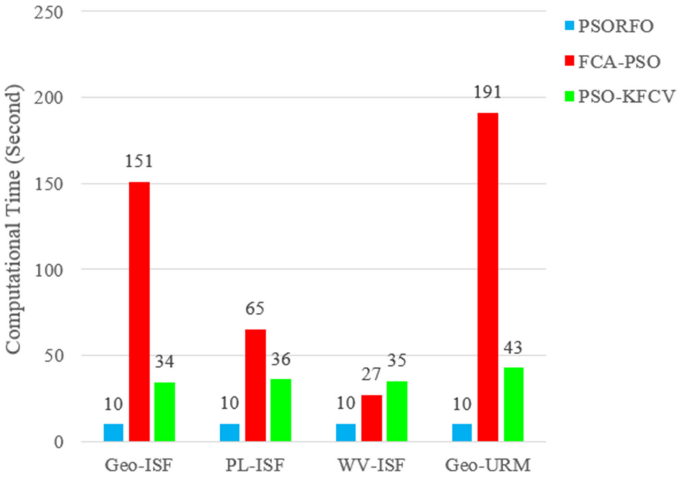

Fig. 3. Average computational time of applying different methods on the experimental data sets.

for the WV-ISF data set. The reason for this is that the WV-ISF data set is a small subset of its original image and, as a result, its GDEM and extracted points from that are small. In summary, it may be concluded that FCA-PSO, due to its dependency on GDEM size, has the worst computational time. On the other hand, PSORFO and PSO-KFCV are not dependent on image size because they do not use GDEM. Compared to PSORFO, PSO-KFCV is 27 s slower on average in the four data sets. However, it may still be considered the best solution, since unlike the PSORFO, it leads to reasonable results, e.g., subpixel accuracy for all the data sets.

IV. Conclusion

Highly correlated RPCs, which cause ill-posedness of RFM equations, noticeably reduce the accuracy of the georeferencing of HRSIs. To address this problem, the innovative method of PSO-KFCV was proposed to select and estimate RPCs through the integration of KFCV and PSO algorithm. The PSO-KFCV method, with the generalization of the CF, stabilizes the results for the distribution of GCPs and different initial values.

Our experiments, conducted on the four HRSIs, demonstrated the superiority of the proposed PSO-KFCV with respect to the competing methods, PSORFO and FCA-PSO. The main advantages of PSO-KFCV are low sensitivity to the changing initial values and GCPs distribution and, also, good functionality in the presence of limited GCPs. Furthermore, unlike the cutting-edge PSO-based method for the georeferencing of HRSIs, i.e., FCA-PSO, the PSO-KFCV does not need any additional data (like GDEM) and has lower computational time.

Acknowledgment

The authors would like to thank Prof. M. J. Valadan Zoej, from KNT University of Technology, for providing some data sets in our case studies. The authors also thank Mr. S. H. Alizadeh Moghaddam for sharing their source code of the FCA-PSO for comparison studies.

References

[1] P. I. Dowman, K. Jacobsen, P. G. Konecny, and R. Sandau, *High Resolution Optical Satellite Imagery*, Scotland, U.K.: Whittles Publishing. 2012.
[2] Y. He and Q. Weng, *High Spatial Resolution Remote Sensing : Data, Analysis, and Applications*. Boca Raton, FL, USA: CRC Press, 2018.
[3] M. Valadan Zoej, M. Mokhtarzade, A. Mansourian, H. Ebadi, and S. Sadeghian, "Rational function optimization using genetic algorithms," *Int. J. Appl. Earth Observ. Geoinf.*, vol. 9, no. 4, pp. 403–413, 2007.
[4] S. Yavari, M. J. Valadan Zoej, A. Mohammadzadeh, and M. Mokhtarzade, "Particle swarm optimization of RFM for georeferencing of satellite images," *IEEE Geosci. Remote Sens. Lett.*, vol. 10, no. 1, pp. 135–139, Jan. 2013.
[5] T. Long, W. Jiao, and G. He, "RPC estimation via l_1-norm-regularized least squares (L1LS)," *IEEE Trans. Geosci. Remote Sens.*, vol. 53, no. 8, pp. 4554–4567, Aug. 2015.
[6] S. H. Alizadeh Moghaddam, M. Mokhtarzade, and S. A. Alizadeh Moghaddam, "Optimization of RFM's structure based on PSO algorithm and figure condition analysis," *IEEE Geosci. Remote Sens. Lett.*, vol. 15, no. 8, pp. 1179–1183, Aug. 2018.
[7] X. Yuan and X. Lin, "A method for solving rational polynomial coefficients based on ridge estimation," *Geomatics Inf. Sci. Wuhan Univ.*, vol. 33, no. 11, pp. 1130–1133, 2008.
[8] X. Wang, D. Liu, Q. Zhang, and H. Huang, "The iteration by correcting characteristic value and its application in surveying data processing," *J. Heilongjiang Inst. Technol.*, vol. 15, no. 2, pp. 3–6, 2001.
[9] Q. Zhou, W. Jiao, and T. Long, "Solution to the rational function model based on the Levenberg-Marquardt algorithm," in *Proc. 9th Int. Conf. Fuzzy Syst. Knowl. Discovery*, 2012, pp. 2795–2799.
[10] Y. Wu and Y. Ming, "A fast and robust method of calculating RFM parameters for satellite imagery," *Remote Sens. Lett.*, vol. 7, no. 12, pp. 1112–1120, 2016.
[11] L. P. Zhao, F. D. Liu, L. Jian, and W. Wang, "Research on reducing term of higher order in RFM model," *Sci. Surveying Mapping*, vol. 32, no. 4, pp. 14–17, 2007.
[12] Y. Zhang, Y. Lu, L. Wang, and X. Huang, "A new approach on optimization of the rational function model of high-resolution satellite imagery," *IEEE Trans. Geosci. Remote Sens.*, vol. 50, no. 7, pp. 2758–2764, Jul. 2012.
[13] L. Tengfei, J. Weili, and H. Guojin, "Nested regression based optimal selection (NRBOS) of rational polynomial coefficients," *Photogrammetric Eng. Remote Sens.*, vol. 80, no. 3, pp. 261–269, 2014.
[14] S. H. Alizadeh Moghaddam, M. Mokhtarzade, A. Alizadeh Naeini, and A. Amiri-Simkooei, "A statistical variable selection solution for RFM Ill-posedness and overparameterization problems," *IEEE Trans. Geosci. Remote Sens.*, vol. 56, no. 7, pp. 3990–4001, Jul. 2018.
[15] K. Sastry, D. E. Goldberg, and G. Kendall, "Genetic algorithms," in *Proc. Search Methodologies*, 2014, pp. 93–117.
[16] J. Kennedy, "Particle swarm optimization," in *Encyclopedia of Machine Learning*. New York, NY, USA: Springer, 2011, pp. 760–766.
[17] M. Jannati and M. J. Valadan Zoej, "Introducing genetic modification concept to optimize rational function models (RFMs) for georeferencing of satellite imagery," *GIScience Remote Sens.*, vol. 52, no. 4, pp. 510–525, 2015.
[18] S. Yavari, M. V. Zoej, M. Mokhtarzadeh, and A. Mohammadzadeh, "Comparison of particle swarm optimization and genetic algorithm in rational function model optimization," in *Proc. XXII ISPRS Congr.*, Melbourne, Australia, 2012, pp. 281–284.
[19] C. V. Tao and Y. Hu, "A comprehensive study of the rational function model for photogrammetric processing," *Photogram. Eng. Remote Sens.*, vol. 67, no. 12, pp. 1347–1358, 2001.
[20] P. Burman, "A comparative study of ordinary cross-validation, v-fold cross-validation and the repeated learning-testing methods," *Biometrika*, vol. 76, no. 3, pp. 503–514, 1989.
[21] T. Hastie, R. Tibshirani, J. Friedman, *The Elements of Statistical Learning*. New York, NY, USA: Springer, 2001.
[22] M.-R. Chen, X. Li, X. Zhang, and Y. Z. Lu, "A novel particle swarm optimizer hybridized with extremal optimization," *Appl. Soft Comput.*, vol. 10, no. 2, pp. 367–373, 2010.
[23] A. Alizadeh Naeini, S. M. J. Mirzadeh, and S. Homayouni, "Global DEMs to tackle RPC biases and the overfitting phenomenon in high-resolution satellite imagery," *Int. J. Remote Sens.*, vol. 39, pp. 6949–6968, Apr. 2018.

Authors' photographs and biographies not available at the time of publication.